Journal of Physical and Theoretical Chemistry
of Islamic Azad University of Iran, 15 (1) 39-46: Spring 2018
(J. Phys. Theor. Chem. IAU Iran)
ISSN 1735-2126

Theoretical investigation about the adsorption of the Sarin nerve agent on C_{20} fullerene and its boron-doped derivative

Morteza Rouhani[*]

Department of Chemistry, Science and Research Branch, Islamic Azad University, Tehran, Iran

Received August 2018; Accepted October 2018

ABSTRACT

Sarin is a very toxic organophosphorus chemical warfare agent which has been used in different wars. According to an immediate demand of detection, secure approachs to break down this toxic nerve agent, the study on decomposition of sarin achieve significance. In this work, we have made endeavors of discovering an approach to neutralize this hazardous kind by adsorption of this molecule by C_{20} fullerene and its boron doped derivative. The results show that Sarin can form interactions with the C_{20} cage in its neutral state and the interactions can be enhanced significantly by introducing an extra boron atom to the system.

Keywords: C_{20}; fullerene; sensation; Sarin nerve agent; DFT.

INTRODUCTION

Sarin (GB), isopropyl methylphosphonofluoridate ($C_4H_{10}FO_2P$) (Scheme 1), is a chemical warfare agent (CWA). Sarin is a famous nerve agent. Schrader, Ambros, Rüdiger and van der LINde were the discoverers of the Sarin. Sarin is a very toxic organophosphorus compound that prevents the acetylcholinesterase (AChE) enzyme, which plays an important role in the nervous system. Sarin was used in terrorist attacks along the history for example against Japan and in the Iran–Iraq war caused killing and injuring a vast number of people. Therefore, the researchs on sarin are so significant for the target of rapidly detecting and decomposing this toxic agent. The large number of theoretical studies of chemical warfare agents have been done by *ab initio*.

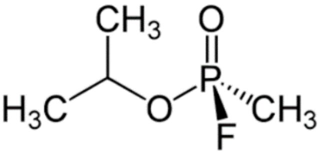

Scheme 1. Sarin nerve agent.

Methods [1,2]. The conformations of sarin, soman and their simulant dimethylmethylphosphonate (DMMP) were completely investigated in vacuum by MP2 theory calculations, along with Fourier transform microwave spectroscopy [3-5]. Kaczmarek et al. [6] studied the very stable conformers of Sarin and Soman in high-level-correlated calculations with extended Gaussian basis sets. Majumdar et al. [7] done conformational analysis of Sarin and Soman at the DFT-B3LYP/6-31++G (d,p) level, comparing their results to MP2/6-31++G** calculations and

---

[*] Corresponding author: rouhani.morteza@gmail.com
morteza.rouhani@alumni.znu.ac.ir

experimental values. Bermudez [8-10] carried out a series of *ab initio* calculations to study Sarin adsorption on different surfaces.

A fullerene also called buckyball is a molecule containing carbon, either in the form of a hollow sphere or an ellipsoid. The first fullerene to be detected was (C_{60}), which was made in 1985. Since the discovery of C_{60} [11,12] doped fullerenes have attracted more interest in vast research fields. Owing to their significant optical, electronic structural and magnetic properties, their potential use has been studied in physics, chemistry, and material engineering [13-16]. One effective usage of these nanostructures is that they can be applied as electrochemical sensors [17-19]. We know that there are various adsorbents used in various aspects. As an example, boron-doped C60 fullerene can be applied for adsorption of CO_2, so it can decrease the global emission of greenhouse gases [20]. Moreover, fullerene C60 has been presented as hydrogen storage [21]. Adsorption of methane on aggregates of C_{60} with positively charge has been studied by computer simulations [22]. It has been shown that calculated adsorption energies have the high-density methane storage on the aggregates of fullerenes. In addition, it has been shown that heteroatom doping or quantum dots capping can efficiently increase the binding energy between adsorbate molecule and nano-substrates [23, 24].

There are three doping methods for forever alerting the charge dispensation and electronic structures of initial fullerenes: The coverage of atoms or ions inside the fullerene cage, the introduction of dopant species around the fullerene, and the replacement of one or more of carbon atoms with dopants. In our mind, there are no computational works to study the nature of interaction between Sarin nerve agent and fullerene (C_{20}) [12]. Now, in this project, we have tried to study the probability of C_{20} fullerene both in adsorption, and in detection of Sarin nerve agent. The results presented in all of the considered cases involving, B doped and the C_{20} fullerene, the adsorption advances via stepwise pathways.

COMPUTATIONAL METHODS

First, the isolated species and dimers were optimized. The possible orientations were then drawn as other input files and putted under additional calculations to give credible geometries. All of the calculations in this study were done by aiding the Gaussian 03 chemical quantum package. The harmonic vibrational frequencies and electronic structures of all stationary points along the reaction pathway were calculated. The Density Functional Theory (DFT) method in Beck's there-parameter hybrid exchange functioning with the correlation functional of Lee, Yang, Parr (B3LYP) [26,27] by applying the 6-311g (d,p) basis set was then applied to optimize the geometries and carrying out the calculations [25]. To evaluate the interaction of GB molecule with fullerene and its boron doped derivative, the correction for BSSE needed to be included in the calculation of adsorption energies. For this purpose, the counterpoise method has been used according to the following equation:

$$E_{\mathrm{ads}} = E_{(\mathrm{Sub\text{-}GB})} - E_{(\mathrm{Sub})} - E_{(\mathrm{GB})} + E_{(\mathrm{BSSE})}$$

where $E_{(\mathrm{Sub\text{-}GB})}$ is the total energy of the substrate (fullerene or its boron doped derivative) interacting with the GB molecule, $E_{(\mathrm{Sub})}$ is the total energy of substrate and $E_{(\mathrm{GB})}$ is the total energy of GB molecule. $E_{(\mathrm{BSSE})}$ is the basis set superposition error (BSSE) which has been calculated using the counter poise method. Counterpoise correction of BSSE decreased the adsorption energy [12].

The electronic density of state DOS was

calculated for the isolated and also for the complex of species to find the sensibility of the C_{20} fullerene toward the Sarin chemical agent. The (NBO) analysis was employed to calculate the electrical charge of each atom in each state, natural bond orbital [29,30]. By using the following formula, the Global Electron Density Transfer (GEDT) was determined [31,32];

$$GEDT = -\Sigma q_A$$

In this formula, q_A is the net Mulliken charge as well as the sum covered the entire atoms of dipolar species [33].

RESULTS AND DISCUSSION

First, each species involving C_{20}, $C_{19}B$ fullerenes and Sarin agent were drawn as input files and optimized separately. In the next step, Sarin molecule was located near to each designed derivative of C_{20} fullerene, in various orientations as input files. During the initial and also the final optimization, some of the different proposed geometries changed to same orientations. So, among various input files, a number of orientations were considered after further optimization process (Fig.1). It has been found that during the calculations, the adsorption process of Sarin was advanced in stepwise pathways for each considered fullerene derivative.

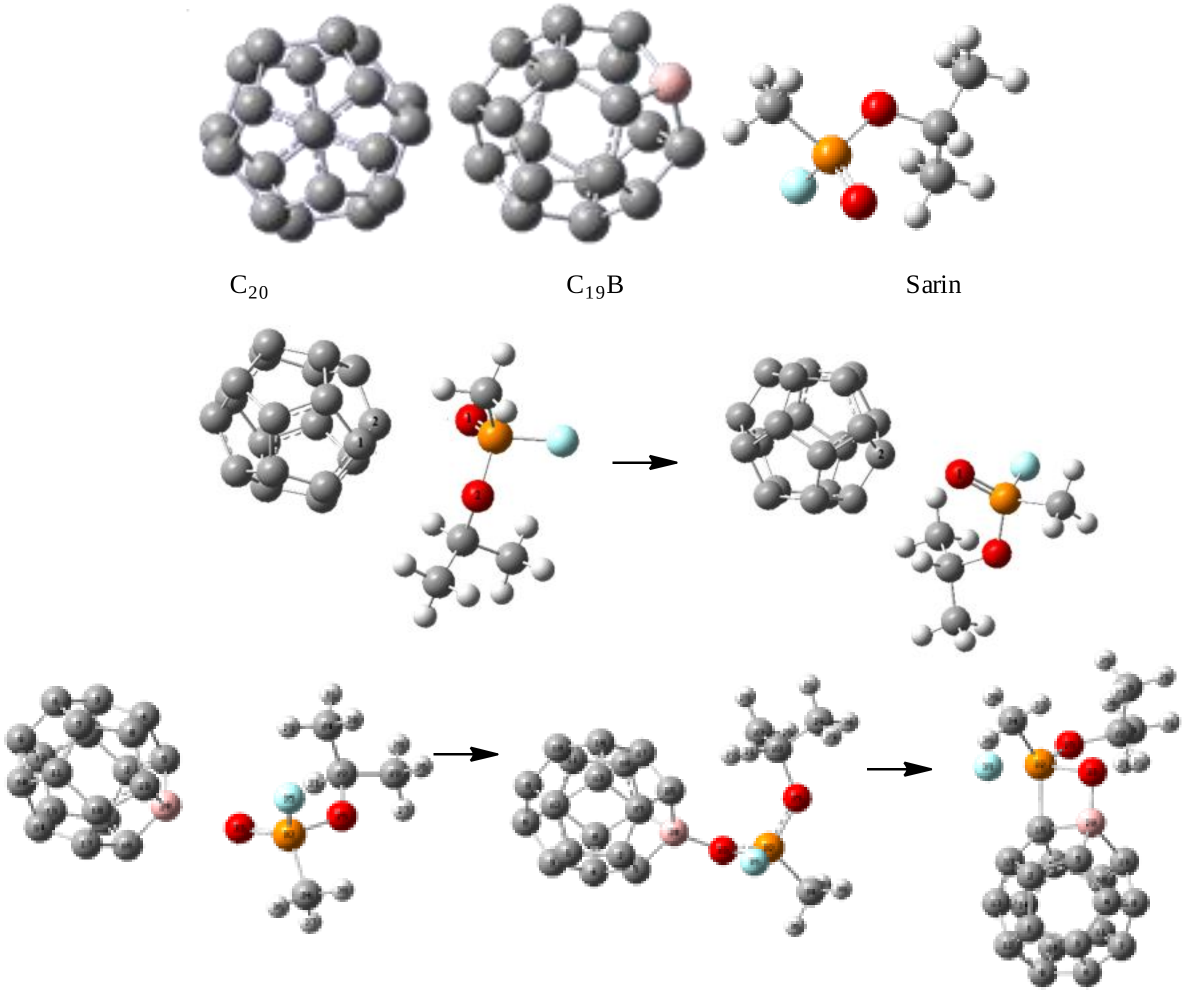

C_{20} $C_{19}B$ Sarin

$C_{19}B$-S $C_{19}B$-S_1 $C_{19}B$-S_2

Fig. 1. The adsorption of Sarin nerve agent by using C_{20} fullerene and its B-doped derivative, optimized at B3LYP/6-311G (d,p) level.

In the case of the adsorption of Sarin by C_{20} fullerene, at the first step adsorption, the ethoxy and carbonyl groups are closed to the fullerene (C_{20}-S) someway, the O1-C2, and O2-C1 lengths are 2.43 Å, and 3.27 Å, respectively. In this condition, the system has an energy content of -8.99 kcal mol^{-1} in comparison with the isolated state and the dihedral angle of C(1)P(2)O(3)C(4) is 160o. After that, a dihedral angle of Sarin turns around P-O bond to C_{20}-S1 in 165o. In that state, the distance between O1 (carbonyl) and C2 of the ring is 2.33 Å (-9.50 kcal mol^{-1} in compression with the isolated state) (Fig. 2).

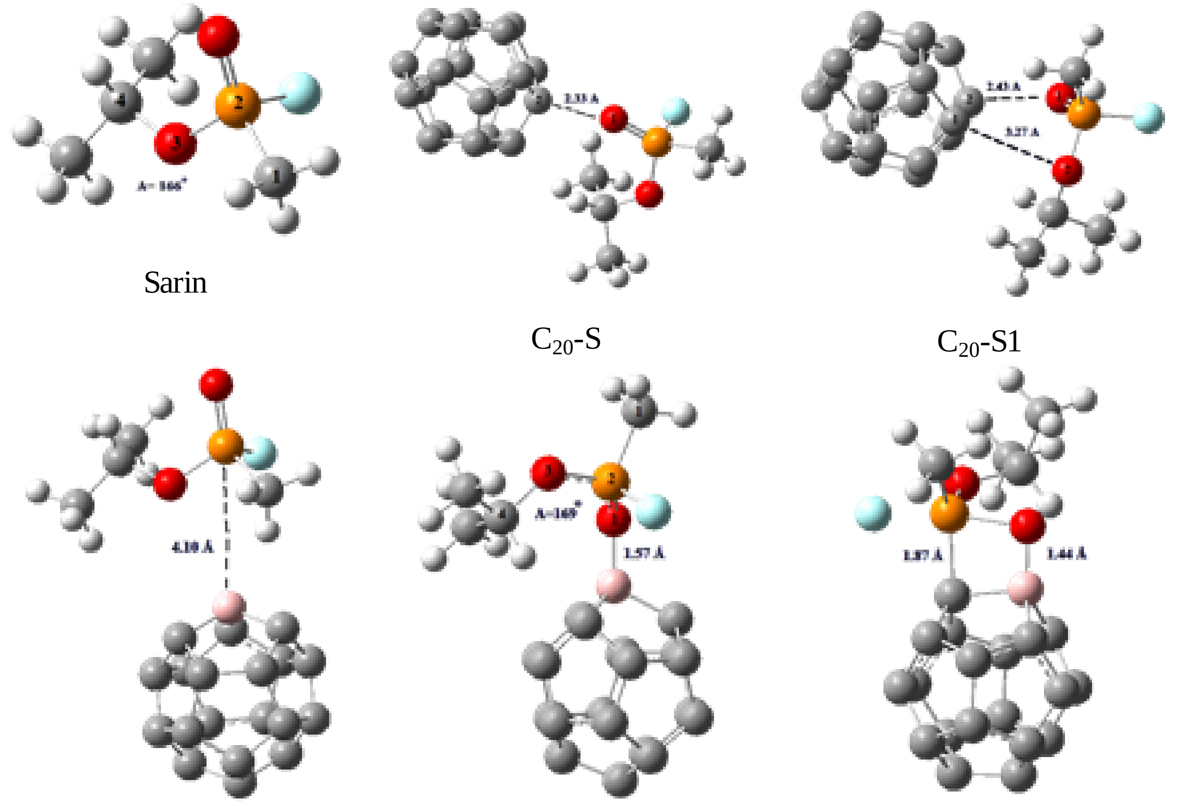

Sarin

C_{20}-S

C_{20}-S1

C_{19}B-S

C_{19}B-S1

C_{19}B-S2

Fig. 2. The detected species for the adsorption of Sarin nerve agent by using C_{20} fullerene and its B-doped derivative, optimized at B3LYP/6-311G (d,p) level.

The adsorption of Sarin, on the surface of C_{19}B fullerene, begins with the constitution of C_{19}B-S system (first step with Eads of -10.00 kcal mol^{-1}), in which no considerable bonding interactions happen between those two species (P-B is 4.10 Å). At the second step (C_{19}B-S1), a strong interaction between the oxygen atom of Sarin (O1) and the boron atom of the fullerene forms (O1- B is about 1.53 Å, see Fig. 2). Another significant change which could be obviously discovered is that C(1)P(2)O(3)C(4) changes from 166o in isolated Sarin, to 169o in C_{19}B-S1. In the final step, the oxygen atom of P=O makes a σ bond with the boron atom of fullerene that leads to destruction of Sarin (C_{19}B-S2). The potential energy of this system is considerably lower than the former adsorption step (-55.61 kcal mol^{-1})

which demonstrates the decomposition of Sarin seems to be very desirable.

In order to investigation of the changes of the electronic structure of C_{20} fullerene and its B-doped derivative, made by the adsorption of Sarin, the net charge transferred (Q) between each of the fullerenes and Sarin was calculated with the aid of Mulliken charge analysis. Charge transfer has an important role in the electronic characteristics and stability of an interacting system. Moreover, the positive values demonstrated the charge transfer from Sarin to fullerene, and the negative values correspond to charge transfer from fullerene to Sarin in all cases. The global electron density transfer in the C_{20}-S system was -0.066 e^- (in position one) and 0.09 e^- (in position to; C_{20}-S1) according to the Mulliken charge analysis. It demonstrates that in both positions, Sarin does not send or receive a significant Mulliken charge value; but, in the second position (C_{20}-S1), the charge transfer and also the molecular orbital interactions between those two species are more than in position one (C_{20}-S). In the issue of adsorption of Sarin in the surface of C_{19}B, at the first adsorption step, the amount of charges which were transferred from Sarin to the fullerene is +0.005 which shows a weak molecular orbital interaction between those two species. At the second step (C_{19}B-S1), the charge transfer increases to +0.355 e^- which is due to the strong interaction between the oxygen atom of Sarin and the boron atom of the fullerene. At the third (final) step of adsorption, Sarin decomposes on the surface of fullerene and make new covalent bonds with the carbon atoms of C_{20} (0.449 e^-).

The results given in Table 1, and Fig. 1, show that doping a Boron atom on the structure of C_{20} fullerene would result in a stepwise adsorption process of Sarin agent, which it finally leads to the destruction of this. Fig. 1 shows the adsorption mechanism of Sarin nerve agent proceeds via a multistep channel. For C_{20} fullerene, the first step adsorption energy which leads to C_{19}-S geometry is about -8.99 kcal mol^{-1}; while, the second step adsorption energy, is about -9.50 kcal mol^{-1} which belongs to C_{20}-S1 system. We examined different possible orientations between C_{20} and Sarin molecules. However, only two mentioned spices (C_{20}-S and C_{20}-S1) are at lower minima. Because, there is no possible other significant interaction between the C_{20} and Sarin molecules, further input files for the decomposition of Sarin on the surface of C_{20} fullerene did not optimized truly; while, in other case (C_{19}B), the adsorption of Sarin gas, led to destruction of this molecule (see C_{19}B-S2 sate in Fig. 1).

Table 1. Calculated values for the energy for the adsorption (E_{ads}) of Sarin on C_{20} derivatives, the *GEDT* indices, the HOMO energy (E_{HOMO}), the LUMO energy (E_{LUMO}), and the HOMO-LUMO energy gap (E_g)

System	Eads (kcal mol^{-1}) Non-corrected	E_{BSSE}	Eads (kcal mol^{-1}) Corrected	GEDT	EHOMO (eV)	ELUMO (eV)	Eg (eV)
C_{20}	---	---	---	---	-0.219	-0.126	-0.093
C_{20}-S	-9.04	0.05	-8.99	-0.066	-0.256	-0.122	-0.134
C_{20}-S1	-9.53	0.03	-9.50	+0.09	-0.241	-0.104	-0.137
$C_1$9B	---	---	---	---	-0.223	-0.125	-0.098
C_{19}B-S	-10.02	0.02	-10.00	+0.005	-0.231	-0.120	-0.111
C_{19}B-S1	-36.31	0.05	-36.26	+0.355	-0.255	-0.126	-0.129
C_{19}B-S2	-55.63	0.02	-55.61	+0.449	-0.246	-0.093	-0.153

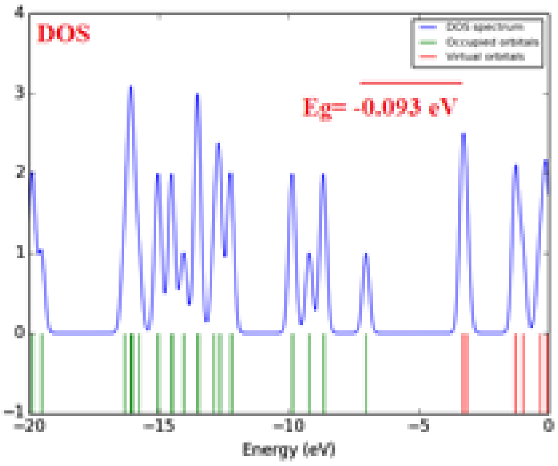

C_{20}

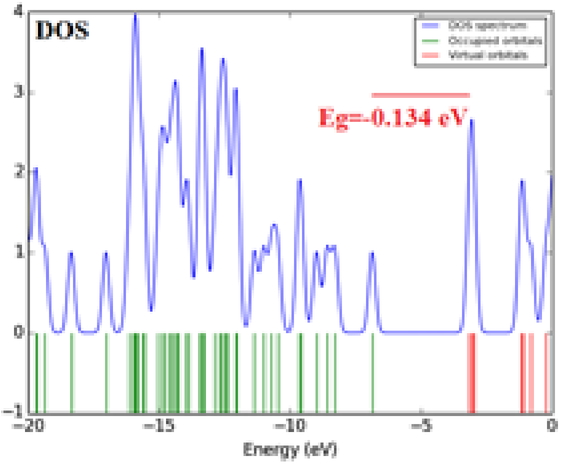

$C_2$0-S1

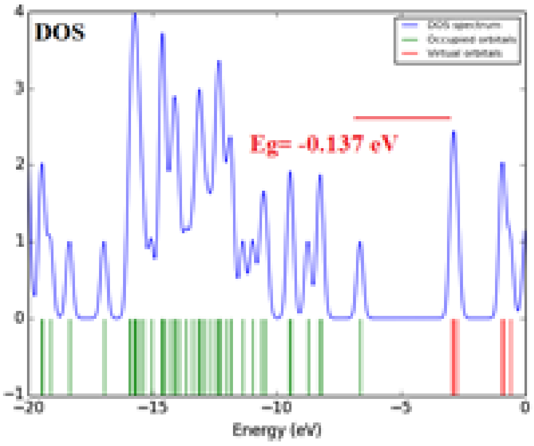

C_{20}-S2

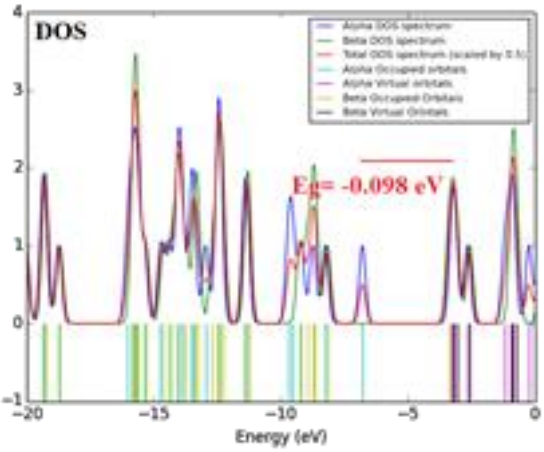

C_{19}B

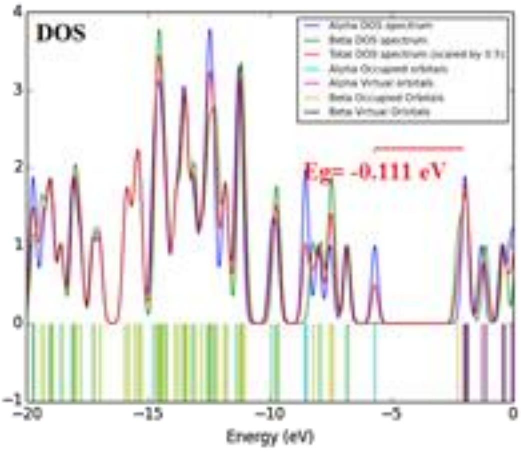

C_{19}B-S

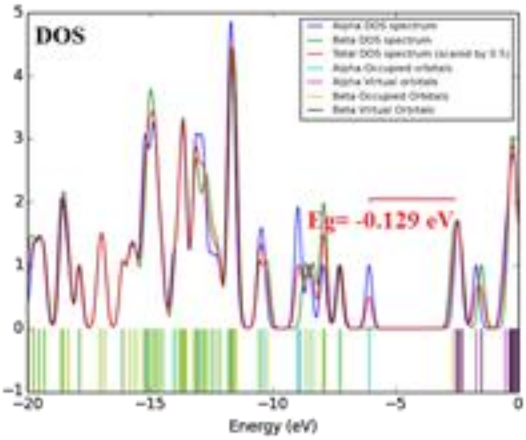

C_{19}B-S1

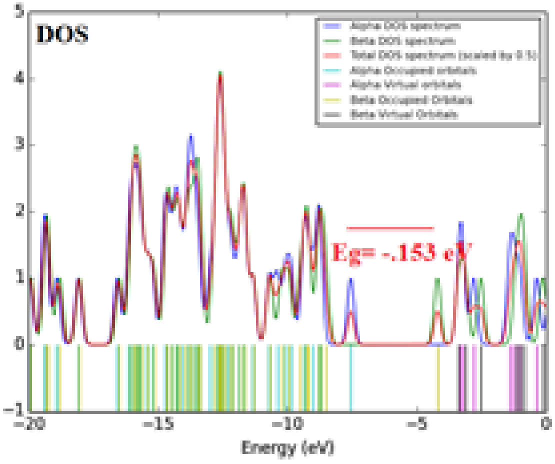

$C_{19}B$-S2

Figure 3. The prepared density of state DOS plots for detected systems optimized at B3LYP/6-311G (d,p) level.

In the case of $C_{19}B$ fullerene, the adsorption mechanism seems to be proceeded via a three-step mechanism. Somehow, at the first step, Sarin approaches to the fullerene with adsorption energy of -10.00 kcal mol^{-1} ($C_{19}B$-S), at the second step, the oxygen atom of P=O bond make an interaction with the boron atom of the fullerene ($C_{19}B$-S1, Eads = -36.26 kcal mol^{-1}). And at the third (final) step of adsorption, Sarin decomposes on the surface of the fullerene to make the $C_{19}B$-S2 system (E_{ads} = -55.61 kcal mol^{-1}).

CONCLUSION

In summary, we have investigated the interaction between the nerve agent, Sarin (GB), and fullerene (C_{20}) as well as its boron doped derivative using the DFT method. The adsorption energy values and equilibrium distances for various adsorption states were calculated, and it was found that the GB molecule adsorbs onto the boron doped derivative with greater affinity than on pure fullerene. Probably, the GB is physisorbed on fullerene, while its adsorption on the boron doped derivative from O and P heads has a chemical nature. In that case, a partial positive charge was developed on boron atom, and was delocalized by O-P=O functional group in GB. As a result, GB is chemisorbed on boron doped derivative, contrary to the GB–fullerene interaction, which occurs physically.

ACKNOWLEDGEMENTS

The author thanks, Islamic Azad University, Science and Research Branch for the support and guidance.

REFERENCES

[1]. M.–T., A. Vishnyakov, G.Y. Gor, A.V. Neimark, J. Phys. Chem. B, 115 (2011) 13617.
[2]. N. Sharma, R. Kakkar, J. Comput. Sci., 10 (2015) 225.
[3]. R.D. Suenram, F.J. Lovas, D.F. Plusquellic, A. Lesarri, Y. Kawashima, J.O. Jensen, A.C. Samuels, J. Mol. Spectrosc., 211 (2012) 110.
[4]. R.D. Suenram, R.S. DaBell, A.R.H. Walker, R.J. Lavrich, D.F. Plusquellic, M.W. Ellzy, J.M. Lochner, L. Cash, J.O. Jensen, A.C. Samuels, J. Mol. Spectrosc., 224 (2004) 176.

[5]. A.R. Walker, R.D. Suenram, A. Samuels, J. Jensen, M.W. Ellzy, J.M. Lochner, D. Zeroka, J. Mol. Spectrosc., 207 (2001) 77.
[6]. A. Kaczmarek, L. Gorb, A.J. Sadlej, J. Leszczynski, Struct. Chem., 15 (2004) 517.
[7]. D. Majumdar, S. Roszakz, J. Leszczynski, Mol. Phys. 105 (2007) 2551.
[8]. V.M. Bermudez, J. Phys. Chem. C, 111 (2007) 9314.
[9]. V.M. Bermudez, J. Phys. Chem. C, 111 (2009) 3719.
[10]. V.M. Bermudez, J. Phys. Chem. C, 113 (2009) 1917.
[11]. H.W. Kroto, J.R. Heath, S.C. O'Brien, R.F. Curl, R.E. Smalley, Nature, 318 (1985) 162.
[12]. S. Arshadi, A.R. Bekhradnia, F. Abbasi Alaei, Phosphorous Sulfur Silicon Relat. Elem.,190 (2015) 2051.
[13]. M.S. Dresslhaus, G. Dresslhaus, P.C. Eklund, Science of Fullerenes and Carbon Nanotubes; Academic Press: New York, NY, (1996).
[14]. W. Andreoni, The Physics of Fullerene-Based and Fullerene-Related Materials; Kluwer: New York, NY, (2000).
[15]. R.H. Xie, Handbook of Advanced Electronic and Photonic Materials and Devices, Vol. 9, Nonlinear Optical Materials; Academic Press: New York, NY, (2000).
[16]. H. Keypour, M. Noroozi, A. Rashidi, M. Shariati Rad, Iran. J. Chem. Chem. Eng. 34 (2015) 21.
[17]. B.S. Sherigara, W. Kutner and F. D'Souza, Electroanalysis, 15 (2003) 753.
[18]. T. Rueckes, K. Kim, E. Joselevich, G.Y. Tseng, C. Cheung, C.M. Lieber, Science, 289 (2000) 94.
[19]. M. Anafcheh, R. Ghafouri, Phosphorus Sulfur Silicon Relat. Elem. 189 (2014) 60.
[20]. W.S. Suchitra, D. Aijun, S. Wijitha, G. Yuantong, Beilstein J. Nanotech. 5 (2014) 413.
[21]. O.V. Pupysheva, A. Farajian, B.I. Yakobson, Nano Lett. 8 (2008) 767.
[22]. A. Kaiser, S. Zöttl, P. Bartl, C. Leidlmair, A. Mauracher, M. Probst, S. Denifl, O. Echt, P. Scheier, Chem. Sus. Chem. 6 (2013) 1235.
[23]. S.N. Azizi, M.J. Chaichi, P. Shakeri, A. Bekhradnia, J. Fluores. 23 (2013) 227.
[24]. A.H. Peyghan, M.T. Baei, P. Torabi, S. Hashemian, Phosphorus Sulfur Silicon Relat. Elem. 188 (2013) 1172.
[25]. M.J. Frisch, G.W. Trucks, H.B. Schlegel, G.E. Scuseria, M.A. Robb, J.R. Cheeseman, V.G. Zakrzewski, J.A. Montgomery, R.E. Stratmann, J.C. Burant, S. Dapprich, J.M. Millam, A.D. Daniels, K.N. Kudin, M.C. Strain, O. Farkas, J. Tomasi, V. Barone, M. Cossi, R. Cammi, B. Mennucci, C. Pomelli, C. Adamo, S. Clifford, J. Ochterski, G.A. Petersson, P.Y. Ayala, Q. Cui, K. Morokuma, D.K. Malick, A.D. Rabuck, K. Raghavachari, J.B. Foresman, J. Cioslowski, J.V. Ortiz, A.G. Baboul, B.B. Stefanov, G. Liu, A. Liashenko, P. Piskorz, I. Komaromi, R. Gomperts, R.L. Martin, D.J. Fox, T. T. Keith, M.A. M.A. Al-Laham, C.Y. Peng, A. Nanayakkara, C. Gonzalez, M. Challacombe, P.M.W. Gill, B. Johnson, W. Chen, M.W. Wong, J.A. Andres, C. Gonzalez, M. Head-Gordon, E.S. Replogle, J.A. Pople, Gaussian 03 Inc., Pittsburgh.
[26]. A.D. Becke, Phys. Rev. A, 38 (1998) 3098.
[27]. C. Lee, W. Yang, R.G. Parr, Phys. Rev. B, 371 (1988) 785
[28]. V.B. Delchev, M.V. Nenkova, Acta Chim. Slov. 55 (2008) 132.
[29]. A.E. Reed, L.A. Curtiss, F. Weinhold, Chem. Rev. 88 (1988) 899.
[30]. J.E. Carpenter, F. Weinhold, J. Mol. Struct. (Theochem). 9 (1988) 41.
[31]. L.R. Domingo, RSC Adv. 4 (2014) 32415.
[32]. R. Jasinski, RSC Adv. 4 (2015) 101045.
[33]. S.A. Siadati, E. Vessally, A. Hosseinian, L. Edjlali, Syn. Met. 220 (2016) 606.